

***Interactive comment on “Observations and scaling of tidal mass transport across the lower Ganges-Brahmaputra delta plain: implications for delta management and sustainability” by Richard Hale et al.***

**J. Shaw (Referee)**

shaw84@uark.edu

Received and published: 26 October 2018

This study details field observations of tides and sediment transport in the tidal region of the Ganges-Brahmaputra-Megha Delta system. This research is important because of the dearth of direct measurement in this vast system, and provides first insights about how the delta keeps pace with relative sea level rise, context for recent human-induced changes, and a baseline for proposed large scale water projects. The authors characterize tidal range, tidal prism, and sediment transport at a few key sites on primary and secondary distributary channels in the tidal region of the delta. This

manuscript significantly increases our understanding of this system. I have a few questions, but I think that this paper should be published in ESURF after minor revisions. The sediment concentration and transport data are the most important deliverable to me, but I have a hard time summarizing the findings, because they seem contradictory. Point 1: suspended sediment concentration in a secondary channel increases during the wet season by three fold, indicating a fluvial origin (Figure 2). Point 2: Surveys of net sediment discharge in a primary channel collected over all survey days reveal a net import of sediment (Figure 7), which suggests that sediment transport is primarily dependent on net water discharge, which suggests that freshwater arrival is of secondary importance. However, the flux variation here is also about a factor of three or four (Table 1), consistent with the secondary (BR) channel. I encourage the authors to test the hypothesis that the transport of sediments is really controlled by the same thing in both primary (Shibsa) and secondary (BR) channels. I understand that this is difficult to do given the varying data types, but that is a simpler and more tractable explanation.

## Minor comments

L258: I think that this is a relatively weak reason to ignore bedload. My intuition is that lots of bed material sand can become suspended under achievable shear velocities and contribute to SSC measurements during velocity maxima, and be transported onto secondary channels or islands if there is enough water discharge. I would say you can neglect bedload if there are no bedforms in your multibeam surveys. Otherwise, I think you just need to say that it could be happening, but that it's likely far less than the suspended component and necessarily neglect it from surveys.

L261: I do not know what "tiling observations" means. Perhaps a quick definition is in order.

L339: It took me a minute to figure out that the tidal prisms you are measuring are from integrating the discharge. I imagine prisms as a space filled, which would be impossible to measure. Consider defining how prisms are found.

L459: Total \_annual\_ mass transport

L496: I do not understand how sediment moving through the system could be “almost wholly derived from the river mouth,” but that the flux through the five major tidal channels could be estimated as roughly equal to the sediment flux of the main river (L486-487). I would suspect that there could also be significant re-entrainment of continental shelf or island sediments that were once river derived, but have been in the coastal zone for years or maybe far longer than that. I think that the case for re-entrained sediments can't be disproved here.

L555: led to a reduction in tidal prism... assuming no feedbacks to tidal dynamics, correct?

---

Interactive comment on Earth Surf. Dynam. Discuss., <https://doi.org/10.5194/esurf-2018-66>, 2018.

Printer-friendly version

Discussion paper



***Interactive comment on “Observations and scaling of tidal mass transport across the lower Ganges-Brahmaputra delta plain: implications for delta management and sustainability” by Richard Hale et al.***

**Allison (Referee)**

meadallison@tulane.edu

Received and published: 27 November 2018

The Hale et al. manuscript is a fine addition to the very sparse literature on water and sediment dynamics in the Ganges-Brahmaputra coastal zone. I think the paper, which should be published, could be improved in several ways.

1. The dataset is sparse, which is understandable given the difficult logistical conditions to work in this setting. However, absence in particular of CTD cast data synchronous with the OBS cast data, left a number of questions in my mind about the possibilities of

Printer-friendly version

Discussion paper



water column salinity stratification in the channels during the dry season, and sediment stratification and bed storage and or sediment convergence during both studies at slack periods and seasonally. I realize that the authors can't fully address these issues, but I think some of the questions could be allayed by presenting some of the original data—ADCP transects of velocity magnitude, direction and backscatter intensity, and OBS profiles for these example sections. None of this data that is used to calculate fluxes is presented as is, and, seeing some of it would be beneficial to the reader.

2. The methodology is lengthy. If necessary, it could be split off into a supplementary methods section, that would allow greater detail on some of the data manipulations to arrive at fluxes that were only briefly covered in the existing version.

3. I believe some mention of the potential importance of tropical cyclones needs presenting in the intro and discussion. That is, these large events may have an impact on sediment fluxes in the system that may or may not exceed the seasonal and tidal scale processes. Although there is no data presented here, it should be mentioned as a possible and unresolved control in the system.

4. line 166. OBS's do not measure SSC's, they measure turbidity and have to be calibrated. Hence, while the profiler OBS was calibrated as discussed, how did SSC's get derived for the long-term station at Sutarkhali?

5. line 256. This mentions ignoring bedload transport but, what is neglected is sand transport in suspension (bed material load transport). Since water sampling was not done isokinetically (Niskin), this component was missed or undersampled. It appears from the water flux rates (no adcp velocity profiles shown) that the tidal energies are high enough during max ebb and flood to transport sand. I would mention this caveat to be fair about what you are actually measuring (fine flux).

---

Interactive comment on Earth Surf. Dynam. Discuss., <https://doi.org/10.5194/esurf-2018-66>, 2018.

In Response to R1:

Dear Dr. Shaw, I think your assessment of our major findings is accurate, except that I see no contradiction. In the primary channel, we maintain that tidal stage (i.e., discharge) is the dominant control on suspended sediment concentrations year round, with the introduction of GBM-derived material during the monsoon playing a secondary role. In the smaller channels (e.g., Bhadra), seasonal delivery of new material appears to play a larger role in sediment flux. This introduces the idea of a “discharge threshold” above which seasonal sediment delivery is relatively less important, however future research is required to test this idea.

L258 – Point taken. This sentence was introduced to let the reader know that we are not forgetting about bedload. The revised manuscript will be more explicit.

L261 – Text will be updated to explain that “tiling observations” means repeating the measured time series at 12.4-h increments to improve interpolation/extrapolation accuracy.

L339 – We will make sure to define tidal prisms as the integrated discharge in this context.

L459 – This change will be made.

L496 – We don’t mean to imply that extensive mixing is not happening – quite the opposite. Several studies (e.g., Rogers et al., 2013; Rogers and Overeem, 2017) have demonstrated the presence of a weak, excess-<sup>7</sup>Be signal in sediment accumulating on the mangrove platform during the monsoon season, with mixing/dilution offered as one potential explanation. This comparison was intended to provide the reader with a sense of scale. We have reworded to be more clear about our intended meaning.

L555 – In this case, the “volume reduction” refers to poldered area that would have been flooded by the Shibsra and its distributaries, multiplied by a characteristic flooding depth. We have reworded this as “reduction or redistribution” to clarify.

In response to R2:

Dear Dr. Allison, Thank you for your review of our manuscript. Please consider the following responses to your concerns:

1 - As you mention, field logistics are challenging here, and for most of this research we did not have a profiling CTD at our avail. Anecdotally, we observe sediment laden plumes regularly boiling to the surface during energetic tides in all seasons, suggesting a physically well-mixed system. Shaha and Cho (2016) demonstrate minimal stratification in primary channel (Pussur) regardless of season, although they do indicate that early in the wet season (e.g., July) mixing between Shibsra and Pussur channels (which occurs in the Dhaki) can result in vertical stratification. Wilson et al. (AGU conference 2018) published observations of surface conductivity along a transect extending from the study area to the Bay of Bengal coastline in March 2015 (dry season). They demonstrate a consistent increase from P-32 (~24 mS/cm) to

the coast of the Bay of Bengal ( $\sim 40$  mS/cm), supporting again that water columns are vertically mixed, rather than stratified.

We have included a figure with example ADCP cross-section velocity data, and SSC casts, to further transparency into our method.

2 – We will have added more detail to this calculation in the final version.

3 – Good point. We are well aware of the regional importance of tropical cyclones, and their potential to move sediment. We will update the text to include this discussion.

4 – Thank you for this clarification. In fact, the OBS deployed in the tidal channel was the same instrument used in the dry season field work (again – we were instrument-limited). The calibration was built from the  $>100$  filtered water samples. We have restructured the methods to describe this calibration earlier on.

5 – Thank you. A similar concern was raised by Referee 1, and we invite you to consider our response to them.

1 **Observations and scaling of tidal mass transport across**  
2 **the lower Ganges-Brahmaputra delta plain:**  
3 **implications for delta management and sustainability**  
4

5 Richard Hale<sup>1</sup>, Rachel Bain<sup>2</sup>, Steven Goodbred Jr.<sup>2</sup>, Jim Best<sup>3</sup>

6 <sup>1</sup>Dept. of Ocean, Earth, and Atmos. Sci., Old Dominion University, Norfolk, VA, USA

7 <sup>2</sup>Earth and Environmental Sciences Dept., Vanderbilt University, Nashville, TN USA

8 <sup>3</sup>Departments of Geology, Geography & GIS, Mechanical Science and Engineering and Ven  
9 Te Chow Hydrosystems Laboratory, University of Illinois, Urbana, IL USA

Deleted: Champagne

10  
11 **Abstract**  
12

13 The landscape of southwest Bangladesh, a region constructed primarily by fluvial  
14 processes associated with the Ganges and Brahmaputra Rivers, is now maintained almost  
15 exclusively by tidal processes as the fluvial system has migrated east and eliminated most  
16 direct fluvial input. In natural areas such as the Sundarbans National Forest, year-round,  
17 inundation during spring high tides delivers sufficient sediment that enables vertical  
18 accretion to keep pace with relative sea-level rise. However, recent human modification of  
19 the landscape in the form of embankment construction has terminated this pathway of  
20 sediment delivery for much of the region, resulting in a startling elevation imbalance, with  
21 inhabited areas often sitting >1 m below mean high water. Restoring this landscape, or  
22 preventing land loss in the natural system, requires an understanding of how rates of water  
23 and sediment flux vary across time scales ranging from hours to months. In this study, we  
24 combine time-series observations of water level, salinity, and suspended sediment  
25 concentration, with ship-based measurements of large tidal-channel hydrodynamics and  
26 sediment transport. To capture the greatest possible range of variability, cross-channel  
27 transects designed to encompass a 12.4-h tidal cycle were performed in both dry and wet  
28 seasons, during spring and neap tides.  
29

Deleted: to the

Deleted: through the Holocene

Deleted: spring-tide

Deleted: for

Deleted: tidal

30 Regional suspended sediment concentration begins to increase in August, coincident with a  
31 decrease in local salinity, indicating the arrival of the sediment-laden, freshwater plume of  
32 the combined Ganges-Brahmaputra-Meghna rivers. We observe profound seasonality in  
33 sediment transport, despite comparatively modest seasonal variability in the magnitude of  
34 water discharge. These observations emphasize the importance of seasonal sediment  
35 delivery from the mainstem rivers to this remote tidal region. On tidal time-scales, spring  
36 tides transport an order of magnitude more sediment than neap tides in both the wet and  
37 dry seasons. In aggregate, sediment transport is flood-oriented, likely a result of tidal  
38 pumping. Finally, we note that rates of sediment and water discharge in the tidal channels  
39 are of the same scale as the annually averaged values for the Ganges or Brahmaputra  
40 rivers. These observations provide context for examining the relative importance of fluvial  
41 and tidal processes in what has been defined as a quintessentially tidally influenced delta in  
42 the classification scheme of Galloway (1975). These data also inform critical questions  
43 regarding the timing and magnitude of sediment delivery to the region, which are  
44 especially important in predicting, and preparing for, responses of the natural system to  
45 ongoing environmental change.  
46

Deleted: somewhat

Deleted: ,

Deleted: indicating

Deleted: this

Deleted:

Deleted: the

Deleted: future change under

Deleted: changing

Deleted: conditions



62  
63  
64  
65  
66  
67  
68  
69  
70  
71  
72  
73  
74  
75  
76  
77  
78  
79  
80  
81  
82  
83  
84  
85  
86  
87  
88  
89  
90  
91  
92  
93  
94  
95  
96  
97  
98  
99  
100  
101  
102  
103  
104  
105  
106

## 1 - Introduction

The world's great deltas are currently threatened by a variety of factors, including global sea level rise (Overeem and Syvitski, 2009), overpopulation (Ericson et al., 2006), changes in sediment supply (Syvitski 2003; Syvitski and Milliman, 2007; Anthony et al., 2015; Darby et al., 2016; Best, 2019), and other human-related activities such as water diversions, flood control structures, and groundwater and hydrocarbon extraction (Syvitski et al., 2009). The Ganges-Brahmaputra-Meghna (GBM) delta is one of the most heavily populated regions that is undergoing locally accelerated sea-level rise (~0.5 cm/y; Higgins et al., 2014) due to a combination of natural and anthropogenic factors including eustatic sea-level change, tectonic subsidence, fine-grained sediment compaction, and groundwater extraction (Overeem and Syvitski, 2009; Syvitski, 2008; Steckler et al., 2010). In addition, when factors such as tidal amplification due to anthropogenic reworking of the distributary channel network are considered, the relative rate of sea-level rise can exceed 1.6 cm/yr (Pethick and Orford, 2013). Furthermore, the future viability of the delta is threatened by the proposed construction of dams and water diversions associated with India's National River Linking Project, which, if completed as proposed, could drastically reduce sediment delivery to Bangladesh (Higgins et al., 2018).

Restoration of land-surface elevation in many populated areas in the GBM delta is already necessary due to the relative loss in elevation that has occurred since the widespread construction of embankments during the 1960s to 1980s. Both planned (tidal river management) and unplanned (embankment failures) flooding of local polders (the embanked islands) has demonstrated the capacity of the natural system for effective sediment transport and deposition, with decimeters of annual accretion observed during recent breach events (Khadim et al., 2013; Auerbach et al., 2015; Kamal et al., 2017; Darby et al., 2018). One of the most important strategies that has been forwarded to reduce the threat of unintended inundations in SW Bangladesh is a plan for polder management (Brammer, 2014). However, many questions concerning potential management strategies remain, not the least of which are an accurate quantification of total available sediment mass and an understanding of the tidal processes involved in its transport and deposition. Toward these goals, the present study provides observation-based calculations of water and sediment transport through a major tidal channel in the delta across spring-neap tidal cycles and seasonal time scales, with the goal of identifying the timing and magnitude of mass sediment exchange between the different tidal channels. Not considered in the present study are the potential impacts of tropical cyclones, which directly impact Bangladesh 0.3-1.5 times per year (Murty et al., 2986; Alam et al., 2003; Saha and Khan, 2014), and can significantly affect the local landscape (Auerbach et al., 2015). The results presented herein are considered in the context of prior research concerning sediment accumulation and rates of channel infilling to better understand the role of tidal mass transport within the lower GBM delta plain.

## 2 - Background

Deleted: like

Deleted: the India

Deleted: rapidly and drastically

Deleted: These

Deleted: results

Deleted: then

113 Much of the low-lying coastal region of SW Bangladesh is under threat of long-term  
114 inundation (Auerbach et al., 2015; Brown and Nicholls, 2015). The risk is particularly acute  
115 for islands that were embanked (“poldered”) in the 1960s and 1970s as part of a program  
116 designed to increase the area of arable land through the prevention of tidal inundation in  
117 agricultural areas (Islam, 2006; Nowreen et al., 2014). Approximately 5000 km of polder  
118 embankments were built by hand, generating 9000 km<sup>2</sup> of new farmland, but also  
119 eliminating the semi-diurnal exchange of water and sediment between the tidal channels  
120 and tidal platform (Islam, 2006; Nowreen et al., 2014). As a result, sediment resupply  
121 pathways have been effectively terminated and the former floodplain surface in these  
122 regions now lies 1.0-1.5 m below mean high water due to a combination of sediment  
123 starvation, enhanced compaction, and tidal-range amplification (Auerbach et al., 2015;  
124 Pethick and Orford, 2013).

Deleted: sediment

125  
126 In contrast to the poldered landscape, the adjacent mangrove system of the Sundarbans  
127 National Forest (SNF) is primarily inundated during spring high tides, and its  
128 sedimentation and vegetation are keeping pace with sea-level rise (Rogers et al., 2013;  
129 Auerbach et al., 2015). Protecting the SNF is of critical importance, as coastal wetlands and  
130 mangroves provide irreplaceable ecosystem services including storm-surge buffering  
131 (Uddin et al., 2013; Marois and Mitsch, 2015; Hossain et al., 2016; Sakib et al., 2015),  
132 serving as effective carbon traps (McLeod et al., 2011; Alongi, 2012; Pendleton et al., 2012)  
133 and perhaps even helping to combat the impacts of ocean acidification (Yan, 2016).  
134

Deleted: ;

Deleted:

135  
136 For the GBM delta, a unit-scale analysis of mass balance (Rogers et al., 2013) suggests that  
137 the annual sediment load of the GBM river system (~1.1 Gt/y) is sufficient to aggrade the  
138 entire delta system at rates  $\geq 0.5$  cm/yr, and thus provides potential to keep pace with  
139 moderately high rates of sea-level rise. Such aggradation, of course, requires effective  
140 dispersal of riverine sediment to disparate regions of the delta. Recent research suggests a  
141 close coupling of discharge at the river mouth to sediment deposition in the remote delta  
142 plain by way of tidal exchange (Allison and Kepple, 2001; Rogers et al., 2013; Auerbach et  
143 al., 2015; Wilson et al., 2017). Such tidally supported sedimentation yields mean accretion  
144 rates of ~1 cm/yr, with local observations regularly reaching 3-5 cm/yr, which together  
145 indicate robust sediment delivery to the Sundarbans and SW coastal region (Rogers et al.,  
146 2013; [Rogers and Overeem, 2017](#)). Thus, as the principal conduit for sediment that can  
147 maintain the elevation of this region, an understanding and quantification of the tidal water  
148 and sediment exchange is essential to foresee future impacts of accelerated sea-level rise  
149 and the potential for mitigation.

Deleted:

### 150 3 – Methods

#### 151 3.1 – Study Area

152 Our research concerns a network of tidal channels located approximately 80 km from the  
153 coast along the Pussur River system, itself one of five similarly sized tidal distributary  
154 networks (Fig. 1). Tidal exchange extends >120 km inland of the coast along the Pussur  
155 River, with one branch ultimately connecting to the Gorai River, a distributary of the  
156 mainstem Ganges River (Fig. 1). The tidal range along the Pussur River approaches its  
157 maximum in the study area at 4-5 m for the spring tidal range, as compared with 3-3.5 m  
158

163 on the coast at Hiron Point. The area is also societally relevant, lying at the transition from  
164 the pristine Sundarbans forest to the embanked polders, and near the formerly active  
165 shipping port of Mongla and cyclone- and flood- impacted island of Polder 32 (labelled P32  
166 on Fig. 1; Auerbach et al., 2015).

167  
168 Within this area, our observations were collected in the primary tidal channel of the Shibsa  
169 River and two of its major bifurcations that connect with the Pussur channel, the Dhaki  
170 River and Bhadra River (Fig. 1). The Shibsa River is the largest of these channels, with local  
171 widths of 1-2 km, compared to 0.25-0.8 km and 0.15-0.3 km, for the Dhaki and Bhadra  
172 Rivers, respectively. At its eastern extent, the Dhaki River connects to the Pussur River,  
173 serving as the first major cross-channel to link the Shibsa and Pussur River channels after  
174 they bifurcate ~60 km to the south (Fig. 1). At its upstream extent, the Pussur tidal channel  
175 connects with the downstream mouth of the Gorai River, which delivers a water discharge  
176 of ~3000 m<sup>3</sup>/s during the monsoon season and decreasing to ~0 m<sup>3</sup>/s during the dry  
177 season (Winterwerp and Giardino, 2012). Salinity in the study area ranges from 0-1 PSU  
178 during the monsoon, to 20-30 PSU during the dry season (Shaha and Cho, 2016; Ayers et  
179 al., 2018). This seasonal variation in salinity is controlled by local runoff, freshwater  
180 discharge from the Gorai River, and to a much larger extent, the magnitude of the regional  
181 discharge plume of the GBM rivers (Rogers et al., 2013).

Deleted: the

### 182 183 3.2. - Hydrodynamic Observations

184  
185 To establish tidal stage and capture surface-water elevations during the hydrodynamic  
186 surveys, pressure sensors were deployed at multiple locations across the study area (Fig.  
187 1). All sensors were deployed as close to low water as possible and recorded at 5- or 10-  
188 minute intervals. Periods of subaerial sensor exposure (of up to 150 minutes at low tide)  
189 were interpolated using a robust ordinary least-squares method provided by Grinsted  
190 (2008). The agreement between measurement and prediction was generally good, with  
191 predicted range being 0.98 of the measured range for a given time period, thus suggesting  
192 that the interpolated data are both reasonable and conservative. The values reported  
193 herein are of the interpolated values. Tidal range, water temperature, and conductivity  
194 have also been monitored continuously since 2014 at the Sutarkhali station (Fig. 1B), with  
195 an optical backscatter sensor (OBS) calibrated to measure suspended sediment  
196 concentration (SSC) added in late March 2015. Prior to deployment in the tidal channel,  
197 this OBS was used to measure vertical profiles of SSC on the Shibsa River, with  
198 simultaneous water samples being collected to calibrate the instrument response to SSC.  
199 Water samples were filtered using pre-weighed 0.4-µm nitrocellulose filters and washed  
200 with freshwater to remove salts. The filters were then dried overnight and re-weighed to  
201 determine the volume-concentration of sediment. The OBS measurements were calibrated  
202 by comparing the voltage response observed in the field with the measured concentrations  
203 from the same time and location, in a method modified from Ogston and Sternberg (1999).  
204 Correlation between filtered samples and instrument voltage was strong, with an average  
205 r-squared value of 0.83±0.1. While the sediment concentrations recorded by this near-bed  
206 instrument are not directly comparable to the depth-averaged measurements made during  
207 the present cross-channel surveys, we herein use these data to extend our understanding  
208 of system behavior between the dry and monsoon seasons. For broader context, data from

210 the sensors deployed at the Sutarkhali station are also compared to monthly averaged  
211 water discharge for the Ganges and Brahmaputra rivers for the period 1980-2000, based  
212 on data from the Bangladesh Water Development Board, and Ganges River sediment  
213 discharge data digitized from Lupker et al. (2011).

214  
215 To quantify water and sediment flux in this area of the tidal transport system, cross-  
216 channel hydrodynamic surveys were conducted during spring and neap tidal conditions at  
217 two transects on the Shibsa River during the dry (March 2015) and wet  
218 (August/September 2015) seasons. An additional wet season transect was also conducted  
219 during moderate tides on the Pussur River. On the Shibsa River, the southern transect was  
220 located south of the poldered landscape and entirely within the confines of the [Sundarbans](#)  
221 [forest](#) (Fig.1). The northern transect was located ~12 km upstream in the poldered region,  
222 just south of the Dhaki-Shibsa confluence and adjacent to Polder 32 to the east and Polder  
223 10-12 to the west (Fig. 1B). Two secondary channels are present between these transect  
224 locations that divert water onto the Sundarbans tidal platform and associated creek  
225 network. Dry season surveys at both the southern and northern transects took place during  
226 peak neap (15-16 Mar) and spring (21-22 Mar) tides. During the ensuing monsoon season,  
227 spring tides were measured on August 30-31 (southern transect) and September 2  
228 (northern transect), followed by neap tides on September 7 and 8 (northern and southern  
229 transects, respectively). Surveys lasted for 11-13 hours as conditions allowed,  
230 encompassing approximately one-half of a tidal cycle (i.e., one high and one low tide).  
231 Because this system is largely semi-diurnal with a minimal mixed component, we are  
232 confident that this time interval was long enough to [accurately](#) describe the system  
233 dynamics.

234  
235 The surveys were conducted using Sontek M9 multi-frequency ADCPs to collect flow-  
236 perpendicular observations of current velocity and direction. Data were collected at 1 Hz,  
237 using both 1.0 and 3.0 MHz transducers, resulting in vertical bins ranging in height from  
238 0.1-1.0 m. From these values, total discharge was calculated by integrating velocity over  
239 space and time. River conventions are used for presenting velocity and discharge data,  
240 where positive values refer to the ebb or downstream direction and negative values for the  
241 flood or upstream transport. A typical survey day included 50-60 individual river crossings  
242 at the transect location, measuring cumulative discharge in both directions across the  
243 channel. [Examples of cross-channel transects of velocity and SSC used to compute](#)  
244 [instantaneous water and sediment discharge can be found in Figure 2.](#) Because surveys  
245 could only be conducted during daylight hours and as weather conditions allowed,  
246 discharge is interpolated to complete a 12.4-hour tidal cycle, which is the average tidal  
247 cycle duration in the area (range: 11.9-13.1 h). By assuming that the change in tidal prism  
248 is negligible between consecutive tides, as suggested by the similarity in tidal elevations  
249 ([Fig. 3](#)), we can tile measurements in 12.4 h increments and interpolate using a cubic  
250 spline. Working conditions were particularly challenging during the monsoon season,  
251 resulting in especially short-duration survey days. In the absence of measured discharge,  
252 we use a mass balance approach to constrain the magnitude of the missing tidal prism data.  
253 For the monsoon-season spring tides, we treat the region between the southern and  
254 northern transects and the southern Bhadra River as a closed system with no long-term  
255 (>1 semidiurnal period) water storage. Using measured Bhadra River discharge values and

Deleted: SNF

Deleted: accurately

Deleted: '

Deleted:

Deleted: Fig. 2

261 assuming a negligible to slightly southerly-directed net flux through the adjacent  
262 Sundarbans, allows us to determine the likely range of values for the unmeasured ebb  
263 prism at the southern transect. For the monsoon-season neap tides, we consider the larger  
264 region bounded by the southern transect to the southwest, the Pussur River below the  
265 Dhaki River confluence to the southwest, and the Bangladesh Water Development Board  
266 gauging station at the Gorai Railway Bridge ~275 river km to the north. Balancing the  
267 measured net flux through the Pussur River and the recorded upstream discharge of the  
268 Gorai River of 3000 m<sup>3</sup>/s with the measured ebb prism at the southern transect allows us  
269 to estimate the missing southern transect flood prism. We then repeated this spring tide  
270 procedure to estimate the unmeasured neap flood prism at the northern transect.

### 272 3.3 – Sediment Observations

274 In addition to water discharge, observations of SSC along the transect lines were made  
275 using a combination of filtered water samples and optical-backscatter (OBS)  
276 measurements. While the exact sampling method varied depending on available  
277 instrumentation and river conditions, the general approach involved collecting OBS  
278 profiles to the maximum possible depth (<10 m), at either two (northern transect) or three  
279 (southern transect) locations along the channel edges and centerline (Figs 1, 2). OBS  
280 measurements were supplemented by simultaneous water samples (100-200 ml) collected  
281 from various depths using a Niskin sampler, which were used to calibrate the OBS as  
282 described above (Section 3.1).

284 In order to calculate total sediment fluxes, the vertically and horizontally distributed SSC  
285 observations collected for each channel cross-section were averaged to produce a series of  
286 temporally discrete SSC values over the course of one tidal cycle (Figs 2, 4). This spatial  
287 averaging appears suitable because the variance was considerably smaller than the  
288 temporal variability associated with tidal discharge and strong seasonal contrasts. Using  
289 wet season data as an example, the average standard deviation of SSC through time at one  
290 sample location was 0.2 g/L, while the average standard deviation of SSC between stations  
291 at any given time was 0.13 g/L. When conditions did not allow samples to be collected at  
292 depths below the water surface, a scaling factor of 1.25 was applied to account for the  
293 higher sub-surface SSC, which we determined by the relationship between depth-averaged  
294 concentrations and surface concentrations from the other available data. Similarly,  
295 measurements from 15 March (dry-season neap tide) were only collected at depths of 5  
296 and 15 m and were thus scaled by a factor of 0.81 to be comparable to other measurements  
297 that included surface SSC values.

299 An important caveat for all SSC measurements is that we present data collected primarily  
300 from the upper water column and not sampled isokinetically, due to instrument limitations  
301 and high current velocities. Thus, our values principally represent suspended load and do  
302 not account for bedload transport, which likely represents an additional component of total  
303 sediment transport. As with our water-discharge measurements, SSC values were  
304 calculated over an entire tidal cycle by repeating a measured time series in 12.4-hour  
305 increments, then interpolating using a cubic spline. From these values, the integrated

Deleted: Fig.

Deleted: . Water samples were filtered using pre-weighed 0.4- $\mu$ m nitrocellulose filters and washed with freshwater to remove salts. The filters were then dried overnight and re-weighed to determine the volume-concentration of sediment. The OBS measurements were calibrated by comparing the voltage response observed in the field with the measured concentrations from the same time and location, in a method modified from Ogston and Sternberg (1999). Correlation between filtered samples and instrument voltage was strong, with an average r-squared value of 0.83 $\pm$ 0.1.

Deleted: the

Deleted: because

Deleted: are dealing mostly

Deleted: with

Deleted: and

Deleted: ing

Deleted: ,

Deleted: what we are referring primarily to measuring

Deleted: is primarily

Deleted: or fine flux,

Deleted: we

Deleted: are largely ignoring the

Deleted: component

Deleted: . While this

Deleted: is presumably a measurable

Deleted: the

Deleted: ,

Deleted: bedload is likely unable to exit the tidal channels during platform irrigation

Deleted: challenging field conditions preclude our ability to directly measure it, and as such is not considered an important source of sediment for land construction. ...

Deleted: of water discharge

Deleted: tiling observations

Deleted: segments

Deleted: and

345 product of water discharge and SSC yields net sediment flux, which we compute using the  
346 time series for each component as calculated using the aforementioned methods.

347

348

## 349 4 – Results

350

### 351 4.1 – Long-term Pressure and OBS

352

353 At our long-term station deployed in a secondary tidal channel (Fig. 1), recorded water-  
354 level variations show tidal-period excursions with a range of 1.8 to 4.8 m over the 12  
355 months of observation (Fig. 3). This variance is, of course, driven primarily by the  
356 fortnightly spring-neap tidal cycle, but there is also a seasonal variability showing the  
357 monsoon period to have a reduced tidal range as compared with the dry season. In this  
358 case, the neap tidal range is ~10% less during the monsoon season, and the spring tidal  
359 range is as much ~20% less, accounting for a nearly 1 m difference (3.9 m vs. 4.8 m). This  
360 reduced range in the monsoon season, however, is not manifested in the elevation of high-  
361 tide water levels, which remained largely consistent between seasons. Rather, the  
362 difference is caused by higher water levels during low tide (Fig. 3), which has the effect of  
363 truncating the tidal range and yielding an overall higher mean water level. These higher  
364 low-water levels associated with the monsoon suggest that they are tied to regional  
365 freshwater drainage and discharge. In addition, another contributing factor could be the  
366 seasonally reversing monsoon wind stresses, but such set-up should enhance high water  
367 levels as well, suggesting that they are not the primary cause. Although further research on  
368 this topic is needed, these distinctions are important herein for understanding the behavior  
369 of the tidal delta plain, as landscape elevations in this region are closely tied to mean high-  
370 tide water levels, and not mean sea level (Auerbach et al., 2015). Thus, as first  
371 demonstrated by Pethick and Orford (2013), the monthly mean tide-gauge data often used  
372 to track seasonal to interannual variations in water level may have relatively little bearing  
373 on the tidal inundation period and sedimentation rates that control tidal platform elevation  
374 (Rogers et al. 2013).

375

376 The arrival of fully fresh water (wet-season) conditions occurs in July, following the peak in  
377 Brahmaputra River water discharge, and roughly coincident with peak Ganges River water  
378 discharge (Fig. 4). Coupled with our long-term pressure gauge, the OBS sensor recorded  
379 relatively constant, but low, mean SSC from the late dry season into the early monsoon  
380 period (late March through July), with weak but noticeable spring-neap variability ranging  
381 from ~0.01 g/L to 0.20 g/L (Fig. 3). However, moving into peak monsoon season, SSC  
382 increases markedly from early August through September, concurrent with the Ganges  
383 River sediment discharge peak (Figs 2, 3). Individual measurements regularly exceeded  
384 0.50 g/L during this time, with maxima >2.5 g/L (Fig. 3). SSC variability around the semi-  
385 diurnal tide and spring-neap cycles was greatly enhanced compared with that during the  
386 dry season, with SSC values during spring tidal cycles exceeding those observed during  
387 neap conditions by a factor of 2-10. By the end of observations in October 2015, SSC began  
388 to drop to levels similar to those observed in mid-August (0.01-1.0 g/L; Fig. 3), but on  
389 average remained well above those of the dry season. For comparison, the mean annual  
390 SSC of the mainstem Ganges-Brahmaputra river is ~1 g/L, and depth-averaged values in

Deleted: :

Deleted: Fig. 2

Deleted: Fig. 2

Deleted: Fig. 3

Deleted: Fig. 2

Deleted: Figs.

Deleted: Fig. 2

Deleted: Fig. 2

399 the main estuary mouth and on the inner shelf commonly range 2-5 g/L during high river  
400 discharge (Barua et al., 1994; Ali et al., 2013). In total, SSC values well in excess of 1 g/L are  
401 regularly observed during the wet season from the mainstem river to the inner shelf and  
402 into the tidal channels of the lower delta plain. These results support previous evidence for  
403 the strong coupling of seasonal river discharge with penecontemporaneous sedimentation  
404 in the remote tidal delta plain (Rogers et al., 2013).

#### 406 4.2 – Hydrography – Water Discharge,

407 Dry season tidal range on the Shibsa River, as measured at Nalian near the northern  
408 transect (Fig. 1B), varied from 2.3 m during the neap minima to 5.6 m during spring  
409 maxima (Fig. 3). The tidal period was slightly longer during neap tides than spring tides  
410 (12.9 h vs. 12.3 h), and the mixed component of the semi-diurnal tide was more  
411 pronounced, with consecutive tidal ranges varying by as much as 0.55 m during neap tides,  
412 versus 0.23 m during spring tides (Fig. 3). During the monsoon fieldwork, the tidal range  
413 was 2.4 and 4.2 m for neap and spring tides, respectively. As with the dry season, total tidal  
414 period during neap tides was slightly longer than spring tides (12.8 h vs. 12.0 h). The mixed  
415 semi-diurnal variability was again greater during neap tides as well, which varied by as  
416 much as 0.25 m, while spring tide variability was typically <0.10 m (Fig. 3).

418 In this study, we calculate the tidal prism by integrating water discharge over the  
419 individual ebb and flood limbs of the tide, with net discharge calculated as the difference  
420 between them. During the dry season, our observations captured both peak flood and ebb  
421 discharges, with interpolation being used over the remaining <5-15% of the tidal cycle (Fig.  
422 5). During the wet season, field conditions during several surveys limited our measurement  
423 to only a partial tidal cycle (~8-9 hr survey; Fig. 5). Only during northern transect spring  
424 tides were conditions favorable for collecting observations of similar duration to the dry  
425 season (~11 hr survey; Fig. 5). Within these limits, however, we have used conservative  
426 interpolation methods to generate error-bound estimates of total water discharge, the  
427 resulting patterns of which provide robust observations concerning system behavior (see  
428 Section 2; Fig. 5).

430 The average tidal-prism magnitudes for the northern and southern transects are  $2.1 \pm 0.7 \times 10^8$   
431  $\text{m}^3$  and  $3.4 \pm 1.4 \times 10^8$   $\text{m}^3$ , respectively. Included in these averages are the absolute  
432 values of flood and ebb tidal prisms measured on spring and neap tides during both wet  
433 and dry seasons (Table 1). Thus, the tidal prism at the northern transect averages only  
434 ~60±10% that of the southern transect regardless of season, even though they are located  
435 just 10 km apart. Most of this difference in discharge (c. 80-100%) can be balanced by  
436 water storage between the two locations, where the product of tidal range and area  
437 between transects is c.  $6.7 \times 10^7$   $\text{m}^3$ . Considering differences in seasonal discharge, results  
438 show that the neap ebb prism is ~30% greater during the monsoon at both transects,  
439 despite having a smaller tidal range compared with the dry season survey. This difference  
440 of  $4-6 \times 10^7$   $\text{m}^3$  equates to an excess ebb discharge of 1800-2800  $\text{m}^3/\text{s}$ , which is about 45-  
441 70% of the mean monsoon discharge of the upstream Gorai River. We thus take the greater

Deleted: :

Deleted: Fig. 2

Deleted: Fig. 2

Deleted: the

Deleted: Fig. 2

Deleted: In order to

Deleted: dry-season

Deleted: the

Deleted: (i.e., integrated

Deleted: discharges

Deleted: t

Deleted: )

Deleted: Fig. 4

Deleted: monsoon

Deleted: challenging

Deleted: resulted in

Deleted: capturing

Deleted: Fig. 4

Deleted: Fig. 4

Deleted: Fig. 4

Deleted: tidal

Deleted: river

465 wet-season ebb prism to simply reflect the addition of local freshwater discharge from the  
466 Gorai River (Table 1; Fig. 1).

467  
468 Strictly speaking, defining a tidal regime as either ebb- or flood- dominant refers to the  
469 water velocity rather than discharge (Pethick, 1980; Brown and Davies, 2010). In the  
470 present study, however, we are interested in the net movement of water and sediment and  
471 thus refer to a particular discharge regime as either ebb or flood “dominated” or “oriented”  
472 based on the net tidal prism (i.e., the difference between ebb and flood discharge). With  
473 this in mind, our surveys suggest that the system varies between ebb and flood orientation  
474 across both tidal phase and season (Table 1). For example, both transects during the dry,  
475 spring and wet, neap surveys show the average ebb-tidal prism to be  $26 \pm 16\%$  larger than  
476 the flood limb. In contrast, the other two survey periods (dry, neap and wet, spring)  
477 yielded balanced to slightly flood dominated tidal prisms ( $9 \pm 8\%$ ). In summary, although  
478 our results on water balance are insufficient for a full understanding of the patterns, a key  
479 finding is that the ebb and flood tidal prisms rarely balance at this location. These tidal-  
480 prism asymmetries appear to be a salient characteristic of the complex, interconnected  
481 channel network of the GBMD tidal delta plain. Thus, even our limited observations require  
482 a lateral (east-west) exchange of water between the Shibsra and parallel Pussur channels  
483 (Fig. 1), which we presume to be driven by locally non-uniform tidal phasing within the  
484 channel network. Given these emergent circulation patterns, it is clear that individual  
485 channels do not operate as closed systems and exhibit local, non-uniform mass exchange,  
486 providing a first indication of how morphologic evolution of [this tidal delta plain and its](#)  
487 [channel network may](#) occur,

488  
489 Although [relative dominance between the ebb and flood tidal prisms](#) [persistently](#) covaries  
490 [\(as described above\)](#), the mean and instantaneous water discharge ( $\text{m}^3/\text{s}$ ) is almost always  
491 flood-dominant (Fig. 6). This circumstance arises from the significant phase shift that  
492 occurs as the tide wave propagates up channel, resulting in a shorter flood period and thus  
493 higher peak discharge. From our measurements of instantaneous discharge across seasons  
494 and tidal conditions, we calculate mean ebb and flood discharges ( $\text{m}^3/\text{s}$ ) for each transect  
495 (Fig. 6). Mean discharge for the northern transect is  $\sim 9100 \text{ m}^3/\text{s}$  on the flood and  $8600$   
496  $\text{m}^3/\text{s}$  on the ebb, and for the southern transect, mean flood and ebb discharges are  $\sim 14,600$   
497 and  $14,200 \text{ m}^3/\text{s}$ , respectively. From these results, we observe that mean discharge at the  
498 northern transect is again  $\sim 61 \pm 1\%$  that of the southern transect, as also recognized for the  
499 tidal prism. Another notable result is that the mean flood discharge ( $\text{m}^3/\text{s}$ ) is 3-6% greater  
500 than on the ebb tide, despite the tidal prism generally being ebb dominant. This disparity is  
501 a function of the shallow-water distortion of the M2 tide, which produces an asymmetrical  
502 waveform with a steeper rising limb than falling limb, and a corresponding reduction in the  
503 duration of the flood tide by  $\sim 60-90$  minutes.

### 504 505 506 **4.3 – Hydrography – Sediment Transport**

507  
508 Suspended sediment measurements collected during the hydrographic surveys show  
509 similar patterns to those of our long-term OBS station. Wet season sediment concentrations  
510 were generally 30-50% higher than during the dry season (Fig. 5). Much greater

Deleted: the

Deleted: s

Deleted: the

Deleted: persistently

Deleted: Fig. 5

Deleted: Fig. 5

Deleted:

Deleted: ing

Deleted: :

Deleted: Fig. 4



521 differences in SSC were observed, however, between neap and spring tidal conditions, with  
522 the latter concentrations being typically ~3 fold greater (0.3-1.5 g/L vs 0.1-0.5 g/L). These  
523 sediment concentrations, coupled with the water discharge observations, were then  
524 extrapolated over the tidal cycle to generate estimates of the rates and magnitude of  
525 sediment transport (Table 1). Results show that integrated sediment transport over a tidal  
526 limb varied by more than an order of magnitude at both transects. Minima of  $0.16 \times 10^8$  kg  
527 (north) and  $0.2 \times 10^8$  kg (south) of sediment exchange were observed during the neap, dry-  
528 season ebb tide, with maxima during spring, monsoon flood tides being an order of  
529 magnitude greater at  $3.3 \times 10^8$  kg (north) and  $3.9 \times 10^8$  kg (south). These values equate to  
530 mean rates of sediment transport ranging from ~700 kg/s during neap, dry season  
531 conditions to ~17,000 kg/s during monsoon-season spring tides. Comparing the ebb and  
532 flood limbs of our surveys, the mean sediment discharge for the ebb tide is 5800 kg/s  
533 compared to 7800 kg/s for the flood tide, demonstrating an overall flood dominance in  
534 sediment transport.

535  
536 These patterns are further supported by the net sediment transport values (i.e., ebb – flood;  
537 Table 1). For a given tidal cycle, net sediment transport was typically  $10^6$ - $10^7$  kg, with  
538 magnitude varying largely with tidal phase, where spring tides generate 1.5 to 3 times  
539 greater net transport than during neap tides (Table 1). Seasonally, net sediment transport  
540 rates were ~30% greater during the wet season, similar to our observations of suspended  
541 sediment concentration. Finally, a comparison of net sediment transport with  
542 corresponding net water discharge shows the two to covary, as expected, with greater net  
543 water discharge resulting in greater net sediment transport (Fig. 7). However, an important  
544 attribute of this relationship reveals a significant bias toward flood-dominant sediment  
545 transport. Data show that even neutral to weakly ebb dominant water discharge yields net  
546 sediment transport in the flood direction (Fig. 7). As noted for water discharge ( $m^3/s$ ), this  
547 disparity is a function of the non-negligible tidal components beyond M2 that result in a  
548 shortened flood limb and extended ebb period (Fig. 3; Table 1). Together, mean sediment  
549 discharge and net sediment transport patterns thus indicate an overall flood-oriented  
550 asymmetry and net onshore transport of sediment.

## 551 552 553 **5 - Discussion**

### 554 555 **5.1 – Relative importance of tides and river**

556  
557 The GBM tidal delta plain comprises a complex channel network that has been little studied  
558 and will require substantial investigation to be understood well. Nevertheless, results of  
559 the current study allow for numerous observations on the scaling and magnitude of tidal  
560 mass transport within this region, establishing a baseline for the role that tides play in  
561 defining the delta system, particularly in the southwest region away from direct fluvial  
562 inputs. To begin, we take an average of the flood and ebb tidal prisms measured at the two  
563 sites on the Shibsra River over both spring and neap tidal phases during wet and dry  
564 seasons, and extrapolate the mean tidal prism over one year. In other words, an average of  
565  $2.7 \times 10^8$   $m^3$  water passes through this region on each of the ~705 tides per year. This basic

Deleted: and

Deleted: of

Deleted: occurred on the spring, monsoon flood tides

Deleted: that range

Deleted: Fig. 6

Deleted: Fig. 6

Deleted: Fig. 2

573 estimation accounts for an average of  $\sim 2 \times 10^{11}$  m<sup>3</sup> of water annually conveyed through  
574 our survey locations, 80 km inland of the coast. Furthermore, this mass exchange is  
575 principally tidal water, as the 50-75% of annual Gorai River discharge captured by the  
576 Shibsra River (i.e.,  $\sim 0.2 \times 10^{11}$  m<sup>3</sup>) accounts for only 10% of the total water exchange  
577 observed for that channel.

578 The significance of these observations from the upstream Shibsra River tidal channel  
579 become more apparent when compared with the mainstem GBM rivers. In this case, the  $\sim 2$   
580  $\times 10^{11}$  m<sup>3</sup> of water conveyed annually through the upper Shibsra River is nearly 20% of the  
581  $\sim 11 \times 10^{11}$  m<sup>3</sup> of total annual water discharge from the entire GBM watershed (Lupker et  
582 al., 2011; Fig. 4). This is an impressive exchange of mass through the upper reaches of a  
583 single tidal channel along the GBM tidal delta plain. For context, the Shibsra River  
584 comprises approximately half (by planform area) of the Pussur River tidal system (Fig. 1),  
585 itself just one of five major tidal drainages along the GBM tidal delta plain (Fig. 1). Taken  
586 together, these basins include  $\sim 10$  tidal channels having similar area (width  $\times$  length) to  
587 the Shibsra River. We take the tidal flow through these systems to be broadly similar given  
588 the linear relationship between peak tidal discharge and the cross-sectional area of large  
589 tidal channels (Rinaldo et al., 1999), plus the fact that land-surface elevation and tidal range  
590 are similar across the region (Chatterjee et al., 2013). Thus, even at a first-order, estimates  
591 of total mass transport across the tidal region would well exceed the  $\sim 11 \times 10^{11}$  m<sup>3</sup> total  
592 volume discharged by the mainstem GBM rivers.  
593

594 The comparable values between our observations of tidal water exchange in this limited  
595 study area and the total freshwater discharge of the GBM rivers demonstrates how tides  
596 hold equivalence in controlling landscape development in the GBMD, which was suggested  
597 as far back as Galloway (1975). To further consider the geomorphic importance of tides to  
598 the GBMD, we make analogous estimations of the sediment transport ( $Q_s$ ) that supports  
599 land-surface aggradation and the dominant water discharge ( $Q_{dom}$ ) that controls tidal  
600 channel morphology (Rinaldo et al., 1999). As done for water discharge, by taking the  
601 average of our tidal hydrography data for sediment transport, we calculate a mean annual  
602 exchange of suspended sediment through the Shibsra River tidal station to be  $\sim 1 \times 10^{11}$  kg  
603 ( $\sim 100$  Mt). For comparison, this estimate of sediment load is roughly 15% of the  $\sim 700$  Mt  
604 of sediment annually discharged to the coast by the GBM rivers (Goodbred and Kuehl,  
605 1999). Thus, if we extrapolate any similar transport value to the other nine GBM tidal  
606 channels, then the sediment exchange through the tidal channels is easily found to be  
607 comparable to the main river mouth. There is, of course, the important caveat that tidal  
608 sediment transport is not unidirectional, and so this integrated exchange of tidal sediment  
609 is not a net flux as it is for river sediment discharge. Nevertheless, the relevant point is that  
610 local, geomorphic reaches of the tidal delta plain have the opportunity for landscape  
611 building through tidal water and sediment exchange at a similar magnitude to the  
612 mainstem GBM rivers. This assertion is not surprising given the relative stability of the  
613 tidal delta plain, which experiences relatively little net erosion ( $\sim 4$  km<sup>2</sup>/yr, or  $\sim 0.02\%$   
614 annual loss; Sarwar and Woodroffe, 2013) and is offset by widespread sediment deposition  
615 on both land-surface (Rogers et al., 2013) and in channels (Wilson et al., 2017).  
616  
617

Deleted: Fig. 3

Deleted: GMB

Deleted: This

Deleted: magnitude

Deleted: of

Deleted: the

Deleted: comparable

Deleted: importance

Deleted: further

Deleted: very

Deleted: ,

Deleted: the

630 From this study, we understand that tidal energy, independent of the main river mouth,  
631 accounts for a twice-daily exchange of a mass equivalent to 4-15% of the yearly averaged  
632 daily GBM river discharge. In primary channels, the magnitude of this exchange is  
633 controlled more by the spring-neap tidal variability than by the seasonal input of new  
634 material (Fig. 5). In the smaller Bhadra tidal channel, on the other hand, SSC variability  
635 demonstrates profound seasonality, presumably because discharge (and therefore stream  
636 power) is at least an order of magnitude smaller here than in the Shibs River. This  
637 disparity is important when we consider land-building processes, as the majority of the  
638 Sundarbans forest is plumbed by tidal channels on the scale of the Bhadra River or smaller.  
639 Storms may also play a role in remobilizing sediment from the shelf onto the tidal  
640 deltaplain, as suggested by Hanebuth et al. (2013) in their study of ancient salt kilns buried  
641 along the coast. However, there are no observations of significant direct storm deposition  
642 from recent cyclones (Aila, 2009 and Sidr, 2007), such as that recognized from the offshore  
643 Bengal shelf and Swatch-of-No-Ground canyon (e.g. Kudrass et al., 1998; 2018; Michels et  
644 al., 1998; Rogers et al., 2015). The potentially limited impact of storms on sedimentation  
645 and the channel network of the tidal deltaplain may be due its frequent and persistent  
646 exposure to high sediment concentrations and strong currents (>3 m/s) driven by the  
647 tides. Nevertheless, future research should aim to quantify storm inputs and their relative  
648 importance upon sedimentation and morphodynamics of the tidal deltaplain.

650 These findings and discussion points emphasize the essential role that tides play in  
651 maintaining the largest portion of the GBM lower delta plain, which is not under direct  
652 river influence. However, despite the essential role of tides in mixing and dispersing  
653 sediment to large areas of the delta, the supply of sediment remains largely  
654 contemporaneous with seasonal fluvial discharge, especially in the secondary and tertiary  
655 channels that irrigate the Sundarbans. Together, the coupled system in which the GBM  
656 rivers deliver sediment that is subsequently redistributed by tidal energy is fundamentally  
657 responsible for sustainability of this region relative to sea-level change (e.g., Angamuthu et  
658 al., 2018). A significant corollary of this fact is that a change in sediment supply from the  
659 GBM rivers, such as that proposed under India's National River Linking Project, could pose  
660 a serious threat to delta sustainability (Higgins et al., 2018; Best, 2019).

662 To summarize, as the central coastal region receives little direct water and sediment  
663 discharge from the GBM, the results herein emphasize that tidal exchange is the dominant  
664 geomorphic agent in the region with a mass and energy exchange of comparable or greater  
665 magnitude to the mainstem rivers. It is, of course, essential to recognize that most  
666 freshwater and sediment exchanged within the tidal system is ultimately sourced by the  
667 main rivers, and that these are intrinsically coupled systems. Thus, continued sustainability  
668 of the region will require the sustained delivery and exchange of water and sediment  
669 between the fluvial and tidal portions of the delta.

## 671 5.2 – Sedimentation in the Sundarbans and Infilling of Tidal Channels

673 Our observations of tidal sediment exchange provide a useful baseline for examining  
674 sedimentation in the Sundarbans and broader tidal delta plain, which are at risk from sea-  
675 level rise and inundation without an adequate supply of sediment. To date, the best

Deleted: rather

Deleted: Fig. 4

Deleted: BR

Deleted: SNF

Deleted: BR

Deleted:

Deleted:

Deleted:

Deleted: the

Deleted: to

Deleted: dispersal

Deleted: almost wholly derived from the river mouth  
and ...

Deleted: SNF

Deleted: the

691 estimate of total sedimentation in the Sundarbans is  $1.1 \times 10^{11}$  kg/year (~100 Mt), based  
692 on one season of direct sedimentation measures at 48 stations across the region (Rogers et  
693 al., 2013). This mass of sediment deposited in the Sundarbans is basically equivalent to the  
694 ~100 Mt of sediment that we observe transported through the Shibsra River transects.  
695 Thus, recalling that our local measurements likely capture just 5-10% of total suspended  
696 sediment transported through the tidal channels of the region, it becomes evident that  
697 there is generally adequate suspended sediment available to support regional  
698 sedimentation in the Sundarbans.

700 Another plausible implication is that there appears to be adequate sediment available for  
701 the restoration of land elevation within the poldered region, which is a major challenge  
702 facing coastal Bangladesh (Amir et al., 2013). Although a definitive answer remains to be  
703 determined, this general assertion is supported by observations of the rapid sedimentation  
704 that occurred on Polder 32 in the two years following the embankment failures caused by  
705 cyclone Aila in 2009 (Auerbach et al., 2015). Measurements at Polder 32 after these  
706 failures found an average of  $37 \pm 17$  cm/yr of tidal sedimentation sustained over its two-  
707 year exposure to tidal inundation, corresponding to a total annual deposition of ~5 Mt.  
708 Based on inundation depth and period, this accounts for an average of ~0.2 g/L of sediment  
709 extracted from the tidal waters that flooded the island during this time. This value  
710 compares to a mean suspended sediment concentration of ~0.6 g/L measured during our  
711 hydrographic surveys, suggesting that roughly one-third of the tidal sediment inundating  
712 the landscape generated these very rapid sedimentation rates. Ultimately, limitations in the  
713 present data preclude a closed, precise sediment budget, but our collective observations  
714 over several different studies remain consistent in direction and magnitude. These indicate  
715 persistent, relatively rapid, rates of deposition that are sustained by the large-magnitude  
716 conveyance of sediment through the tidal channels and ultimately supplied by seasonal  
717 discharge of the mainstem rivers (Rogers et al., 2013; Auerbach et al., 2015; this study).

719 Upstream of our transect sites, the landscape is almost entirely embanked by polder  
720 systems. With limited opportunity for sediment deposition on this formerly intertidal  
721 platform, and with the resulting reduction or redistribution of the tidal prism upstream,  
722 channel sedimentation and infilling has become a major problem. Wilson et al. (2017)  
723 demonstrate that by preventing the inundation of the intertidal platform, poldering has  
724 reduced the tidal prism of the broader southwest region by as much as  $1.4 \times 10^9$  m<sup>3</sup>. If we  
725 assume that this volume reduction is relatively evenly dispersed across the delta plain,  
726 then it would have led to a 25-50% reduction in the local tidal prism measured at our sites.  
727 These effects are at least partially responsible for the ~1400 km of channel infilling that  
728 has taken place over the last few decades, resulting in the creation of new agriculture and  
729 aquaculture opportunities but also altering drainage, transportation routes, and feedback  
730 responses of the regional tidal hydrodynamics (Wilson et al., 2017). The mass of sediment  
731 that has infilled these channels is calculated to be  $6.15 \times 10^{11}$  kg, which would be  $\sim 1.2 \times$   
732  $10^{10}$  kg/yr assuming a roughly constant rate (Wilson et al., 2017). Of these infilled  
733 channels, ~15% (~200 km) are part of the former channel network connecting upstream  
734 of our northern transect (Fig. 1). Thus, a proportional rate of sedimentation lost to these  
735 channels would be  $\sim 0.18 \times 10^{10}$  kg/yr, which is ~25% of the estimated  $0.68 \times 10^{10}$  kg

Deleted: during

Deleted: a

Deleted: period

Deleted: for

Deleted: in

741 fluxing through the northern transect (to the north) each year. While this sediment  
742 [exchange](#) is four times greater than the expected total based on infilling rates from Wilson  
743 et al. (2017), it relies on the same previously described assumptions (i.e., no lateral  
744 exchange with neighboring rivers, non-end-member flux reflecting an average of end-  
745 member conditions). More importantly, it appears that there is sufficient sediment  
746 available to continue infilling channels, and future studies should constrain whether this  
747 region is, in fact, infilling faster than other areas on the tidal delta plain, as this would hold  
748 important implications for regional navigation and hydrodynamic changes.

Deleted: flux

## 750 6 – Conclusions

751  
752 In the present study, we have measured tidal and seasonal variability associated with  
753 water discharge and suspended sediment concentration (SSC), and used these observations  
754 to compute the magnitude of water and sediment exchange through a single tidal channel.  
755 As has been suggested previously, the wet season is found to exert a strong control on the  
756 timing and magnitude of sediment transport in this system, despite seemingly modest  
757 changes to the hydrodynamics. Indeed, despite a reduced tidal range and similar peak SSC,  
758 sediment transport during the monsoon is always of greater magnitude than during the dry  
759 season. Understanding this relationship is critical for planning any potential land recovery  
760 strategies in the future. The importance of the monsoon also provides a new perspective  
761 into the meaning of a “tidal delta.” While it is clearly the tides that perform much of the  
762 work to shape the delta – including driving a net flood-oriented direction of sediment flux –  
763 it is the seasonal influx of riverine sediment that allows this work to continue. Finally, this  
764 research demonstrates that the mass of sediment transported north of our study area is  
765 more than sufficient to fill channels and create additional land. Ideally, future land-use  
766 management strategies [could](#) divert some of this excess sediment into polder interiors  
767 through tidal river management ([e.g., Seijger et al., 2018; Shampa et al., 2012; van Staveren](#)  
768 [et al., 2016](#)), and allow this landscape to continue to prosper.

Deleted: should

### 770 Code availability:

771

### 772 Data availability:

773 Data used for this publication will be archived in the Marine Geoscience Data System.

774

### 775 Sample availability:

776 Samples from this publication are stored in the sedimentology laboratory at Vanderbilt  
777 University

778

### 779 Author Contribution:

780 The experiment was designed by RH and SG, with input from RB and JB. RH and RB led the  
781 field research efforts with support from SG and JB. RH wrote the majority of the manuscript  
782 and figures, with substantial input from SG. RB and JB also contributed to the manuscript  
783 and figures.

Deleted: a

### 785 Competing interests:

786 The authors declare that they have no conflict of interest.

790  
791  
792  
793  
794  
795  
796  
797  
798  
799  
800  
801  
802  
803  
804

**Acknowledgements:**

This work would not be possible without the support of our local collaborators, Drs. Kazi Matin Ahmed and Syed Humayun Akchter from Dhaka University, who oversaw in-country logistics and offer local guidance. We would also like to thank Abu Naser Hossain of the Forestry Crime Department for his help with permitting, and Nasrul Islam Bachchu of Pugmark Tours, and the captain and crew of the M/V Bawali and M/L Mawali for their seemingly endless patience with our field logistics. We would also like to thank Md. Saddam Hossain, Abrar Hossain, Mynul Hassan, Carol Wilson, and Mike Reed for their field support. This research was supported by the US Office of Naval Research (N00014-11-1-0683) and the National Science Foundation (Coastal SEES- #1600319).

Deleted: .  
Deleted: oversee

807 **References:**

- 808  
809 [Alam, M.A., Hossain, M.A., and Shafee S. Frequency of Bay of Bengal cyclonic storms and](#)  
810 [depressions crossing different coastal zones. \*International Journal of Climatology\*, 23,](#)  
811 [pp. 1119-1125, 2003.](#)
- 812 Ali, A., Mynett, A.E. and Azam, M.H. Sediment dynamics in the Meghna estuary, Bangladesh:  
813 A model study. *Journal of Waterway Port Coastal and Ocean Engineering-ASCE*, 133:  
814 255-263, 2007.
- 815 Allison, M. and Kepple, E. Modern sediment supply to the lower delta plain of the Ganges-  
816 Brahmaputra River in Bangladesh. *Geo-Marine Letters*, 21(2), pp.66-74, 2001.
- 817 Alongi, D.M. Carbon cycling and storage in mangrove forests. *Annual Review of Marine*  
818 *Science*, 6, pp.195-219, 2014.
- 819 Amir, M.S.I.I., Khan, M.S.A., Khan, M.K., Rasul, M.G. and Akram, F. Tidal river sediment  
820 management-A case study in southwestern Bangladesh. *International Journal of*  
821 *Environmental, Chemical, Ecological, Geological and Geophysical Engineering*, 7(3),  
822 pp.176-185, 2013.
- 823 [Angamuthu, B., Darby, S.E., and Nicholls, R.J. Impacts of natural and human drivers on the](#)  
824 [multi-decadal morphological evolution of tidally-influenced deltas. \*Proceedings of the\*](#)  
825 [\*Royal Society A\*, 474, 20180396, 2018.](#)
- 826 Anthony, E.J., Brunier, G., Besset, M., Goichot, M., Dussoillez, P. and Nguyen, V.L. Linking  
827 rapid erosion of the Mekong River delta to human activities. *Scientific Reports*, 5,  
828 p.14745, 2015.
- 829 Auerbach, L.W., Goodbred Jr, S.L., Mondal, D.R., Wilson, C.A., Ahmed, K.R., Roy, K., Steckler,  
830 M.S., Small, C., Gilligan, J.M. and Ackerly, B.A. Flood risk of natural and embanked  
831 landscapes on the Ganges-Brahmaputra tidal delta plain. *Nature Climate Change*, 5(2),  
832 p.153, 2015.
- 833 Ayers, J. C., George, G., Fry, D., Benneyworth, L., Wilson, C., Auerbach, L., Roy, K., Karim, M.R.,  
834 Akter, F., Goodbred, S. Salinization and arsenic contamination of surface water in  
835 southwest Bangladesh. *Geochemical Transactions*, 18(1), 4, 2017.
- 836 Barua, D. K., Kuehl, S. A., Miller, R. L., & Moore, W. S. Suspended sediment distribution and  
837 residual transport in the coastal ocean off the Ganges-Brahmaputra river  
838 mouth. *Marine Geology*, 120(1-2), 41-61, 1994.
- 839 [Best, J. Anthropogenic stresses on the world's big rivers. \*Nature Geoscience\*, 12, pp 7-21,](#)  
840 [doi: <https://doi.org/10.1038/s41561-018-0262-x>, 2019.](#)
- 841 Brammer, H. Bangladesh's dynamic coastal regions and sea-level rise. *Climate Risk*  
842 *Management*, 1, pp.51-62, 2014.
- 843 Brown, J.M. and Davies, A.G. Flood/ebb tidal asymmetry in a shallow sandy estuary and the  
844 impact on net sand transport. *Geomorphology*, 114(3), pp.431-439, 2010.
- 845 Brown, S. and Nicholls, R.J. Subsidence and human influences in mega deltas: the case of the  
846 Ganges-Brahmaputra-Meghna. *Science of the Total Environment*, 527, pp.362-374,  
847 2015.
- 848 Chatterjee, M., Shankar, D., Sen, G.K., Sanyal, P., Sundar, D., Michael, G.S., Chatterjee, A.,  
849 Amol, P., Mukherjee, D., Suprit, K. and Mukherjee, A. Tidal variations in the Sundarbans  
850 estuarine system, India. *Journal of Earth System Science*, 122(4), pp.899-933, 2013.

Deleted: review

Deleted: marine

Deleted: s

Deleted: reports

Deleted: earth

Deleted: system

Deleted: science

858 Darby, S.E., Hackney, C.R., Leyland, J., Kummu, M., Lauri, H. Parsons, D.R., Best, J.L, Nicholas,  
859 A.P. and Aalto, R. Fluvial sediment supply to a mega-delta reduced by shifting tropical-  
860 cyclone activity. *Nature*, 539, 276-279, doi:10.1038/nature19809, 2016.

861 Darby, S.E., Nicholls, R.J., Rahman, M.M., Brown, S. and Karim, R. A Sustainable Future  
862 Supply of Fluvial Sediment for the Ganges-Brahmaputra Delta. In *Ecosystem Services for*  
863 *Well-Being in Deltas* (pp. 277-291). Palgrave Macmillan, Cham, 2018.

864 Ericson, J.P., Vörösmarty, C.J., Dingman, S.L., Ward, L.G. and Meybeck, M. Effective sea-level  
865 rise and deltas: causes of change and human dimension implications. *Global and*  
866 *Planetary Change*, 50(1-2), pp.63-82, 2006.

867 Galloway, W.E. Process framework for describing the morphologic and stratigraphic  
868 evolution of deltaic depositional systems in M.L. Broussard, ed. *Deltas: models for*  
869 *exploration*, pp. 87-98, Houston Geological Society, 1975.

870 Goodbred Jr, S.L. and Kuehl, S.A. Holocene and modern sediment budgets for the Ganges-  
871 Brahmaputra river system: Evidence for highstand dispersal to flood-plain, shelf, and  
872 deep-sea depocenters. *Geology*, 27(6), pp.559-562, 1999.

873 Grinsted, A. Tidal fitting toolbox (v 1.3.0.0), Matlab code,  
874 [https://www.mathworks.com/matlabcentral/fileexchange/19099-tidal-fitting-](https://www.mathworks.com/matlabcentral/fileexchange/19099-tidal-fitting-toolbox?s_tid=srchtitle)  
875 [toolbox?s\\_tid=srchtitle](https://www.mathworks.com/matlabcentral/fileexchange/19099-tidal-fitting-toolbox?s_tid=srchtitle), 2008.

876 [Hanebuth, T.J.J., Kudrass, H.R., Linstadter, J., Islam, B., and Zander, A.M. Rapid coastal](#)  
877 [subsidence in the central Ganges-Brahmaputra Delta \(Bangladesh\) since the 17th](#)  
878 [century deduced from submerged salt-producing kilns. \*Geology\*, 41\(9\), pp.987-990,](#)  
879 [2013.](#)

880 Higgins, S.A., Overeem, I., Steckler, M.S., Syvitski, J.P., Seeber, L. and Akhter, S.H. InSAR  
881 measurements of compaction and subsidence in the Ganges-Brahmaputra Delta,  
882 Bangladesh. *Journal of Geophysical Research: Earth Surface*, 119(8), pp.1768-1781,  
883 2014.

884 Higgins, S., Overeem, I., Rogers, K. and Kalina, E. River linking in India: Downstream impacts  
885 on water discharge and suspended sediment transport to deltas. *Elem Sci Anth*, 6(1),  
886 2018.

887 Hossain, M.S., Dearing, J.A., Rahman, M.M, and Salehin, M. Recent changes in ecosystem  
888 services and human well-being in the Bangladesh coastal zone. *Regional*  
889 *Environmental Change* 16(2):429-443, 2016.

890 Islam, M.R. Managing Diverse Land Uses in Coastal Bangladesh: Institutional  
891 Approaches. *Environment and livelihoods in tropical coastal zones*, p.237, 2006.

892 Kamal, A.S.M., Hossain, A., Hossain, B.M., Hassan, S.M. and Rashid, A.K.M. Physical and Social  
893 Assessment of the Waterlogged Area and Suitability of the “Inclusive and Adaptive  
894 Tidal River Management Technique” to Alleviate Waterlogging in Southwest  
895 Bangladesh. *Procedia Engineering*, 212, pp.760-767. , 2018.

896 Khadim, F.K., Kar, K.K., Halder, P.K., Rahman, M.A. and Morshed, A.M. Integrated water  
897 resources management (IWRM) impacts in south west coastal zone of Bangladesh and fact-  
898 finding on tidal river management (TRM). *Journal of Water Resource and*  
899 *Protection*, 5(10), p.953, 2013.

900 [Kudrass H.R., Michels K.H., Wiedicke M., Suckow A. Cyclones and tides as feeders of a](#)  
901 [submarine canyon off Bangladesh. \*Geology\*, 26, pp.715-718, 1998.](#)

Formatted: Font: Italic

Deleted: 18

Deleted: engineering



904 [Kudrass, H.R., Machalett, B., Palamenghi, L., Meyer, I., and Zhang, W. Sediment transport by](#)  
 905 [tropical cyclones recorded in a submarine canyon off Bangladesh. \*Geo-Marine Letters\*,](#)  
 906 [38\(6\), pp.481-496.](#)  
 907 [Lupker, M., France-Lanord, C., Lavé, J., Bouchez, J., Galy, V., Métivier, F., Gaillardet, J.,](#)  
 908 [Lartiges, B., and Mugnier, J.L. A Rouse-based method to integrate the chemical](#)  
 909 [composition of river sediments: Application to the Ganga basin. \*Journal of Geophysical\*](#)  
 910 [Research: Earth Surface, 116, pp.1-24, 2011.](#)  
 911 Marois, D.E. and Mitsch, W.J. Coastal protection from tsunamis and cyclones provided by  
 912 mangrove wetlands—a review. *International Journal of Biodiversity Science, Ecosystem*  
 913 *Services & Management*, 11(1), pp.71-83, 2015.  
 914 Mcleod, E., Chmura, G.L., Bouillon, S., Salm, R., Björk, M., Duarte, C.M., Lovelock, C.E.,  
 915 Schlesinger, W.H. and Silliman, B.R. A blueprint for blue carbon: toward an improved  
 916 understanding of the role of vegetated coastal habitats in sequestering CO2. *Frontiers*  
 917 *in Ecology and the Environment*, 9(10), pp.552-560, 2011.  
 918 [Michels, K.H., Kudrass, H.R., and Hu, C. The submarine delta of the Ganges- Brahmaputra :](#)  
 919 [cyclone-dominated sedimentation patterns. \*Marine Geology\*, 149, pp.133-154, 1998.](#)  
 920 [Nowreen, S., Jalal, M.R. and Khan, M.S.A. Historical analysis of rationalizing South West](#)  
 921 [coastal polders of Bangladesh. \*Water Policy\*, 16\(2\), pp.264-279, 2014.](#)  
 922 Ogston, A.S. and Sternberg, R.W. Sediment-transport events on the northern California  
 923 continental shelf. *Marine Geology*, 154(1-4), pp.69-82, 1999.  
 924 Overeem I. and Syvitski, J.P.M. Dynamics and Vulnerability of Delta Systems: LOICZ Reports  
 925 and Studies, No 35, GKSS Research Center, Geesthacht, 54 p., 2009.  
 926 Pendleton, L., Donato, D.C., Murray, B.C., Crooks, S., Jenkins, W.A., Sifleet, S., Craft, C.,  
 927 Fourqurean, J.W., Kauffman, J.B., Marbà, N. and Megonigal, P. Estimating global “blue  
 928 carbon” emissions from conversion and degradation of vegetated coastal  
 929 ecosystems. *PloS One*, 7(9), p.e43542, 2012.  
 930 Pethick, J.S. Velocity surges and asymmetry in tidal channels. *Estuarine and Coastal Marine*  
 931 *Science*, 11(3), pp.331-345, 1980.  
 932 Pethick, J. and Orford, J.D. Rapid rise in effective sea-level in southwest Bangladesh: its  
 933 causes and contemporary rates. *Global and Planetary Change*, 111, pp.237-245, 2013.  
 934 Rinaldo, A., Fagherazzi, S., Lanzoni, S., Marani, M. and Dietrich, W.E. Tidal networks: 3.  
 935 Landscape-forming discharges and studies in empirical geomorphic  
 936 relationships. *Water Resources Research*, 35(12), pp.3919-3929, 1999.  
 937 [Rogers, K.G., and Goodbred, S.L. Mass failures associated with the passage of a large tropical](#)  
 938 [cyclone over the Swatch of No Ground submarine canyon \(Bay of Bengal\): \*Geology\*,](#)  
 939 [38\(11\), pp.1051-1054, 2010.](#)  
 940 Rogers, K.G., Goodbred Jr, S.L. and Mondal, D.R. Monsoon sedimentation on the ‘abandoned’  
 941 tide-influenced Ganges–Brahmaputra delta plain. *Estuarine, Coastal and Shelf*  
 942 *Science*, 131, pp.297-309, 2013.  
 943 [Rogers, K.G., and Overeem, I. Doomed to drown? Sediment dynamics in the human-](#)  
 944 [controlled floodplains of the active Bengal Delta. \*Elementa: Science of the\*](#)  
 945 [Anthropocene](#), 6, p. 66. doi:10.1525/elementa.250, 2017.  
 946 [Saha, M.K., and Khan, N. Changing profile of cyclones in the context of climate change and](#)  
 947 [adaptation strategies in Bangladesh. \*Journal of Bangladesh Institute of Planners\*, 7, pp.](#)  
 948 [63-78, 2014.](#)

Deleted: one

Formatted: Font: Not Italic

Formatted: Font: Not Italic

Formatted: Font: Not Italic

Formatted: Font: Italic

Formatted: Font: Not Italic

950 Sakib, M., Nihal, F., Haque, A., Rahman, M., & Ali, M. Sundarban as a Buffer against Storm  
951 Surge Flooding. *World Journal of Engineering and Technology*, 3, 59–64, 2015.

952 Sarwar, M.G.M. and Woodroffe, C.D. Rates of shoreline change along the coast of  
953 Bangladesh. *Journal of Coastal Conservation*, 17(3), pp.515-526, 2013.

954 [Seijger, C., Datta, D.K., Douven, W., van Halsema, G. and Khan, M.F. Rethinking sediments,  
955 tidal rivers and delta livelihoods: tidal river management as a strategic innovation in  
956 Bangladesh. \*Water Policy\*. doi: <https://doi.org/10.2166/wp.2018.212>, 2018.](#)

957 Shaha, D.C. and Cho, Y.K. Salt plug formation caused by decreased river discharge in a  
958 multi-channel estuary. *Scientific Reports*, 6, p.27176, 2016.

959 [Shampa, M., and Pramanik, I.M. Tidal River Management \(TRM\) for Selected Coastal Area of  
960 Bangladesh to Mitigate Drainage Congestion. \*International Journal of Scientific and  
961 Technology Research\*, 1\(5\), pp.1–6, 2012.](#)

962 Steckler, M.S., Nooner, S.L., Akhter, S.H., Chowdhury, S.K., Bettadpur, S., Seeber, L. and  
963 Kogan, M.G. Modeling Earth deformation from monsoonal flooding in Bangladesh using  
964 hydrographic, GPS, and Gravity Recovery and Climate Experiment (GRACE)  
965 data. *Journal of Geophysical Research: Solid Earth*, 115(B8), 2010.

966 Syvitski, J.P. Supply and flux of sediment along hydrological pathways: research for the 21st  
967 century. *Global and Planetary Change*, 39(1-2), pp.1-11, 2003.

968 Syvitski, J.P. and Milliman, J.D. Geology, geography, and humans battle for dominance over  
969 the delivery of fluvial sediment to the coastal ocean. *The Journal of Geology*, 115(1),  
970 pp.1-19, 2007.

971 Syvitski, J.P. Deltas at risk. *Sustainability Science*, 3(1), pp.23-32, 2008.

972 Syvitski, J.P., Kettner, A.J., Overeem, I., Hutton, E.W., Hannon, M.T., Brakenridge, G.R., Day, J.,  
973 Vörösmarty, C., Saito, Y., Giosan, L. and Nicholls, R.J. Sinking deltas due to human  
974 activities. *Nature Geoscience*, 2(10), p.681, 2009.

975 Uddin, M. S., van Steveninck, E. D. R., Stuij, M., & Shah, M. A. R. Economic valuation of  
976 provisioning and cultural services of a protected mangrove ecosystem: a case study on  
977 Sundarbans Reserve Forest, Bangladesh. *Ecosystem Services*, 5, 88-93, 2013.

978 [van Staveren, M.F., Warner, J.F., Khan, M.S.A., and Shah Alam Khan, M. Bringing in the tides.  
979 From closing down to opening up delta polders via Tidal River Management in the  
980 southwest delta of Bangladesh. \*Water Policy\*, 19\(1\), pp.147-164, 2016.](#)

981 Wilson, C., Goodbred, S., Small, C., Gilligan, J., Sams, S., Mallick, B. and Hale, R. Widespread  
982 infilling of tidal channels and navigable waterways in human-modified tidal delta plain  
983 of southwest Bangladesh. *Elem Sci Anth*, 5, 2017.

984 Winterwerp, J.C. and Giardino, A. Assessment of increasing freshwater input on salinity and  
985 sedimentation in the Gorai river system. *World Bank Project*, pp.1206292-000, 2012.

986 Yan, W. Can mangroves buffer ocean acidification?, *Eos*, 97, 2016.

987  
988  
989  
990  
991

Deleted: r

Formatted: Font: Not Italic

Formatted: Font: Italic

Formatted: Font: Not Italic

Deleted:

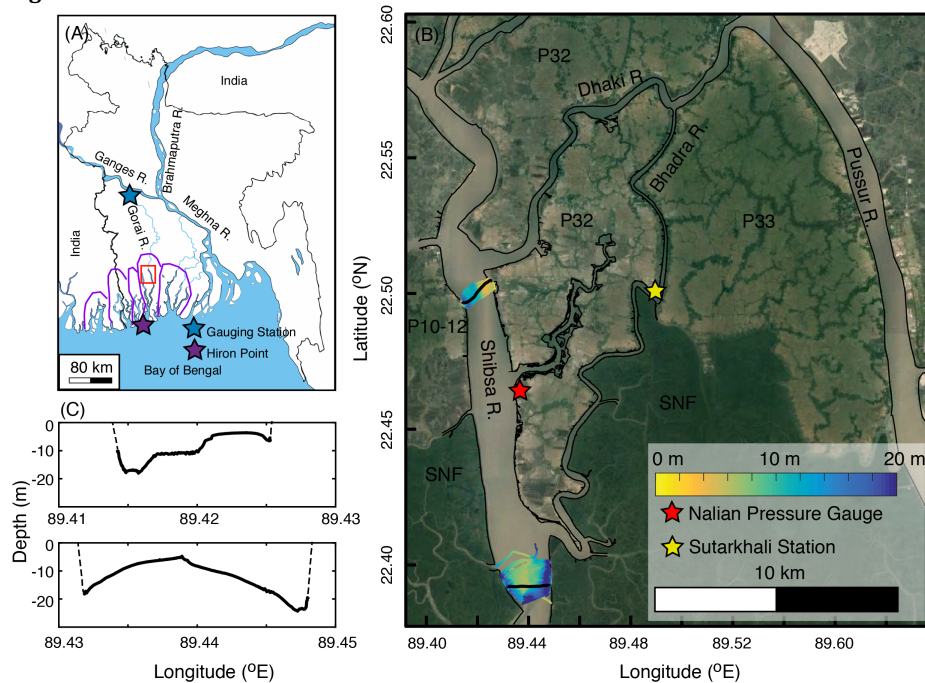
Formatted: Font: Italic

994 Table 1: Measurements of sediment flux and tidal prism from the Shibsra River. Shaded  
 995 rows represent measurements taken during spring tides.  
 996

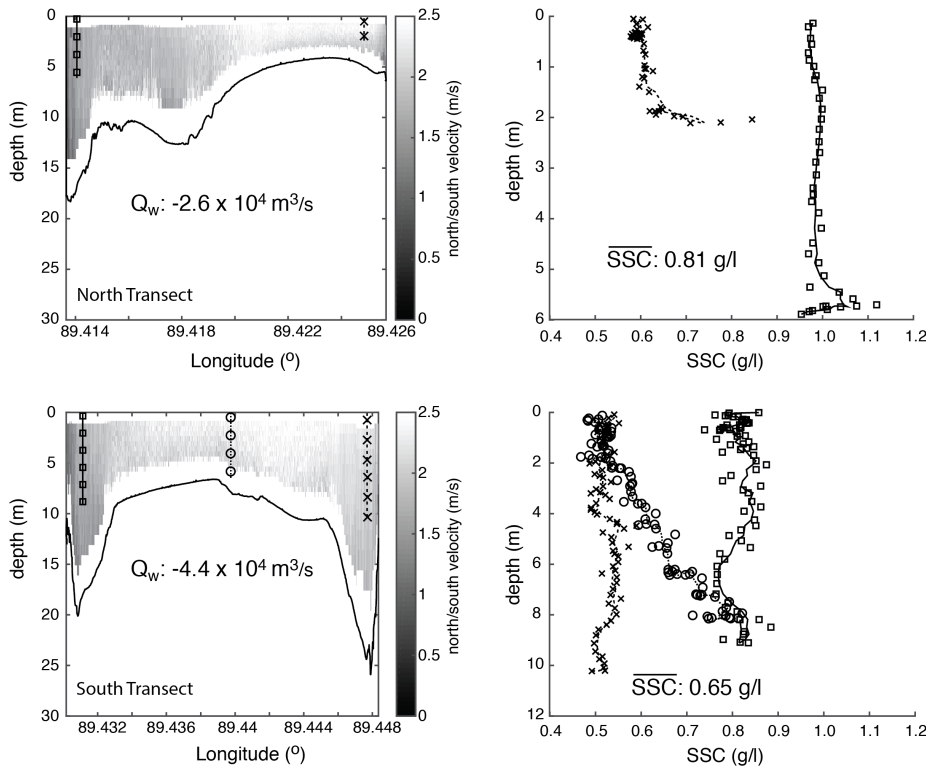
	Transect	Tidal Range (m)	Tidal Prism (m <sup>3</sup> )			Sediment Load (kg)		
			Ebb	Flood	Net	Ebb	Flood	Net
Dry Season	South	2.1	2.00E+08	-2.00E+08	4.30E+05	2.05E+07	-4.70E+07	-2.66E+07
	North	2.2	1.40E+08	-1.50E+08	-1.30E+07	1.55E+07	-2.37E+07	-8.21E+06
	South	5.5	4.50E+08	-4.30E+08	2.30E+07	1.83E+08	-2.30E+08	-4.69E+07
	North	5.7	3.10E+08	-2.30E+08	7.90E+07	2.15E+08	-1.90E+08	2.49E+07
Monsoon	South	2.7	2.64E+08	-1.81E+08	8.28E+07	4.47E+07	-3.89E+07	5.77E+06
	North	2.2	1.83E+08	-1.06E+08	7.69E+07	6.20E+07	-4.12E+07	2.08E+07
	South	4	4.71E+08	-5.12E+08	-4.16E+07	3.20E+08	-3.85E+08	-6.50E+07
	North	3.9	2.40E+08	-2.85E+08	-4.43E+07	2.54E+08	-3.31E+08	-7.65E+07

997  
 998  
 999

1000 **Figures:**

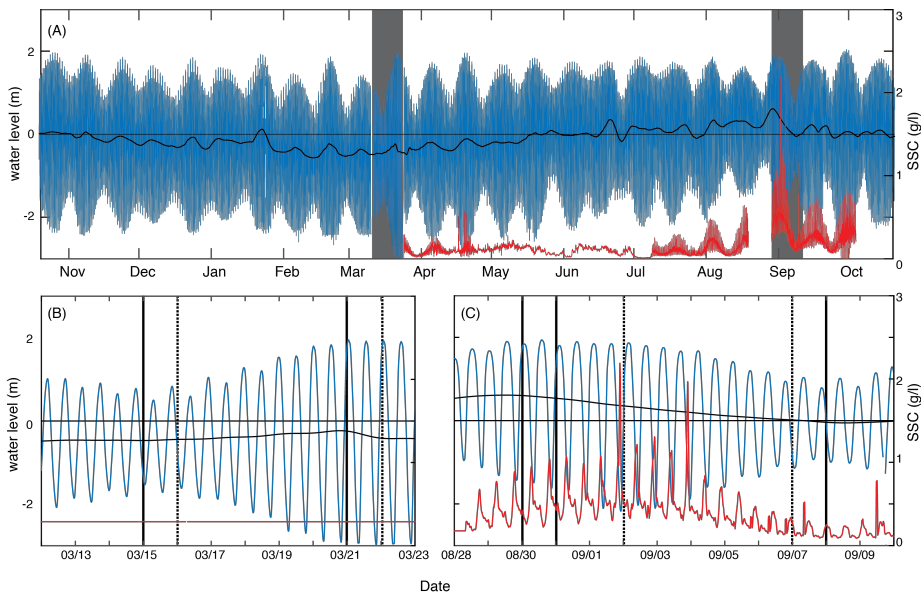


1001 Fig. 1 – A) Location of Bangladesh and the specific region of interest for this study, as well  
1002 as the approximate outlines of the five major tidal distributary basins of the SW delta in  
1003 purple. B) Satellite image of P-32 study area, with bathymetry overlain in the regions of the  
1004 northern and southern transects. Long-term and short-term pressure sensor locations are  
1005 also identified. C) Characteristic river cross sections for the northern and southern  
1006 transects. The specific transects used for these cross sections are highlighted in black in  
1007 (B).  
1008



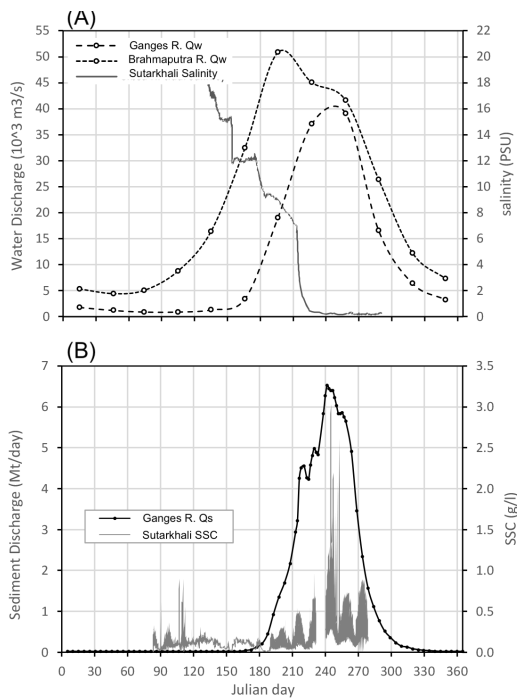
1009  
 1010  
 1011  
 1012  
 1013

Fig. 2 – Example channel cross sections of velocity and SSC collected near maximum ebb-oriented tides during the wet season at the north (top) and south (bottom) transects. Velocity measurements are spatially integrated to compute water discharge. SSC are averaged, with the product of velocity and SSC used to compute sediment discharge.



1014  
 1015 **Fig. 3** – A) Long-term water level elevation (blue) and suspended sediment concentration  
 1016 (red) recorded at Sutarkhali. Black is the tidally filtered water level to highlight seasonal  
 1017 trends of relatively higher water during the monsoon, despite similar maximum tidal  
 1018 elevation. Note also the arrival of increased SSC associated with monsoon discharge of the  
 1019 GBM, beginning in August. Areas shaded in gray depict the periods of focused field work,  
 1020 highlighted below in panels (B) and (C). Days where transect measurements were recorded  
 1021 are noted with vertical black lines, where solid are from the southern transect, and dashed  
 1022 are from the northern transect. In (B), the horizontal red line represents the maximum SSC  
 1023 observed in the spring-neap tidal cycle following our focused field work, as SSC was not  
 1024 measured at this location previously.

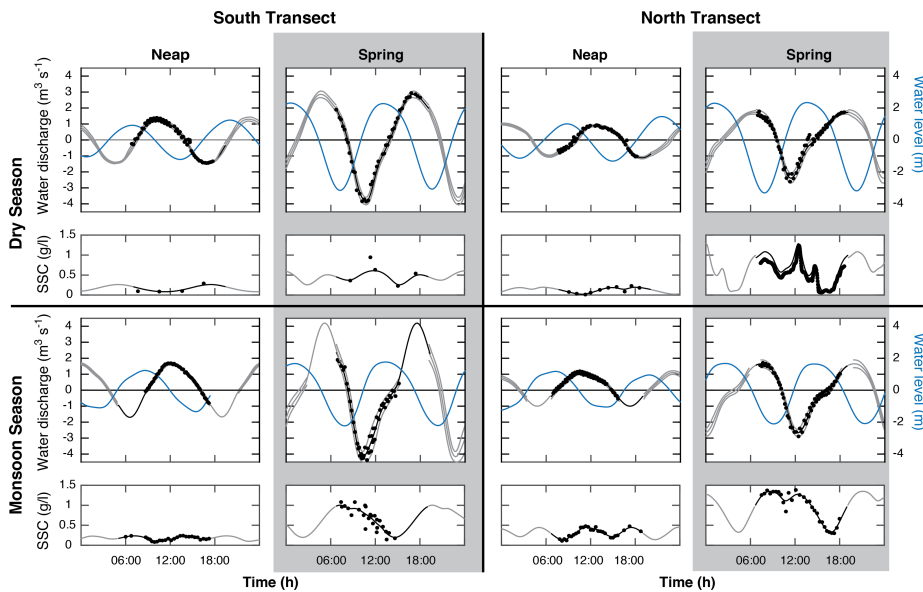
Deleted: Fig. 2



1026  
1027  
1028  
1029  
1030  
1031

Fig. 4 – A) Ganges and Brahmaputra River water discharge ( $Q_w$ ), and salinity measured at Sutarkhali Station, demonstrating the reduction in P-32 salinity associated with the arrival of freshwater from the GBM rivers. B) Ganges river sediment discharge ( $Q_s$ ) interpolated from Lupker et al. (2011) and SSC measured at Sutarkhali station, demonstrating the increase in local SSC coincident with the peak SSC discharge of the Ganges R.

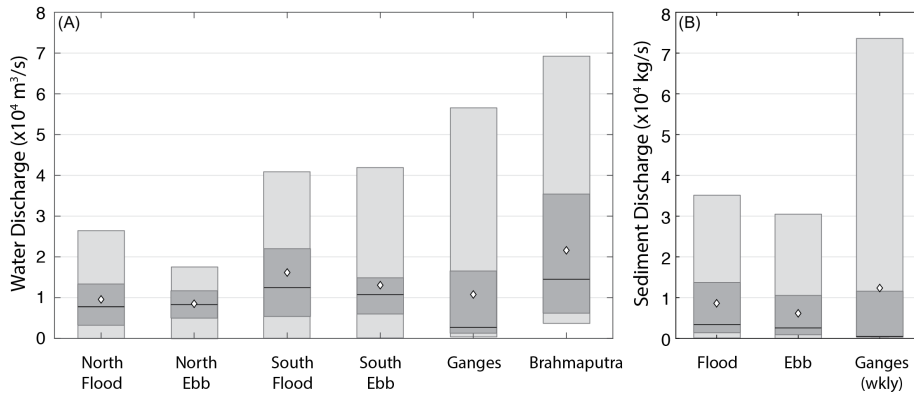
Deleted: Fig. 3



1033  
 1034 **Fig. 5** - Instantaneous water discharge, water level, and depth and width-averaged SSC for  
 1035 each day of cross-channel transects. Dry season measurements are in the upper half, while  
 1036 monsoon season transects are on the bottom. Spring tides in either season are shaded in  
 1037 gray. The two left columns are southern measurements, and the two right columns are  
 1038 from the northern transect. Black dots correspond to specific measurements, while gray  
 1039 lines represent the estimated error, tile forwards and backwards by 12.4 hours. For  
 1040 discharge, dashed lines in the monsoon represent maxima based on extrapolations from  
 1041 the dry season ratio. While seemingly unreasonable, they are provided here for context.  
 1042  
 1043  
 1044

Deleted: Fig. 4

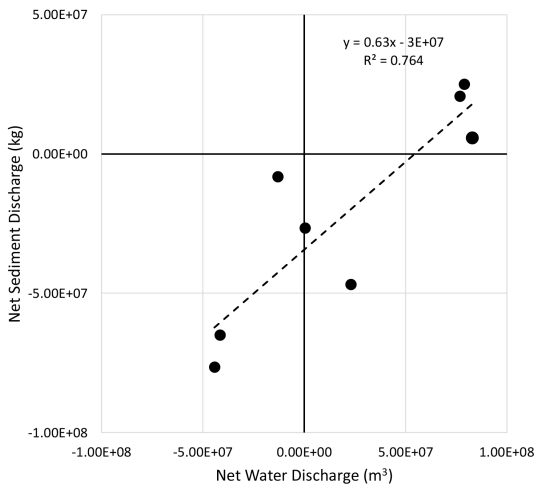




1046  
1047  
1048  
1049  
1050  
1051  
1052  
1053

Fig. 6 – Comparison of mean (diamond), median (black line), 25<sup>th</sup> and 75<sup>th</sup> percentile (lower and upper limits of darkly shaded box) and total range (lightly shaded box) for water discharge (A), and sediment discharge (B). A) demonstrates that median and mean discharge along either transect are comparable to those of either the Ganges or Brahmaputra River. B) demonstrates that as with water, mean sediment discharge on both the flood and ebb tides is approximately the same as the weekly averaged Ganges sediment discharge.

Deleted: Fig. 5



1054  
1055  
1056  
1057  
1058

Fig. 7 – Net water discharge vs. net sediment discharge for all of the survey days on the Shibsra River. As expected, we observe a positive trend to this relationship. The negative y-intercept of the best-fit curve demonstrates the overall flood-oriented nature of sediment transport in this tidal channel.

Deleted: Fig. 6